

2 **Cellulose hydrolysis catalysed by mesoporous activated carbons functionalized under**  
3 **mild conditions**

4 **F.-Z. Azar, M.A. Lillo-Ródenas, M.C. Román-Martínez\***

5  
6 *MCMA Group, Department of Inorganic Chemistry and Materials Institute, Faculty of Sciences, University*  
7 *of Alicante, Ap.99, E-03080 Alicante, Spain*

8  
9 Corresponding author: [mcroman@ua.es](mailto:mcroman@ua.es)

10  
11  
12 **Abstract**

13 The catalytic hydrolysis of cellulose allows the transformation of this sustainable and renewable raw material  
14 to obtain biofuels and high-added value chemicals. The process requires acidic catalysts that should be  
15 preferably solid in order to make it greener, and thus, this work proposes the use of functionalized carbon  
16 materials for such an application. A mesoporous commercial carbon of trade name SA-30, abbreviated as SA  
17 in this work, has been chemically treated at room temperature to create acidic surface oxygen functional groups.  
18 The prepared carbon catalysts have been thoroughly characterized by N<sub>2</sub> adsorption, temperature programmed  
19 desorption (TPD) and X-ray photoelectron spectroscopy (XPS). SAS carbon (prepared by treatment with a  
20 saturated solution of (NH<sub>4</sub>)<sub>2</sub>S<sub>2</sub>O<sub>8</sub> in 1M H<sub>2</sub>SO<sub>4</sub> and named by adding S to the name of the original carbon) is  
21 the most effective of the studied catalysts. It allows achieving high cellulose conversion (about 61%) and  
22 glucose selectivity. Thus, the low-cost functionalized carbons prepared at mild conditions are effective and  
23 promising catalysts for the transformation of cellulose into glucose.

24 **Article Highlights**

25  Activated carbon was modified at mild conditions, identifying and quantifying surface species by XPS and  
26 TPD.

27  Carbon surface species influence selectivity of cellulose hydrolysis into glucose catalysed by activated  
28 carbon

29  Acidic oxygen surface groups positively affect selectivity of cellulose conversion to glucose

30 **Keywords:** Cellulose hydrolysis; Glucose; Carbon materials; Room temperature functionalization.

31 **M.A. Lillo-Ródenas. ORCID: 0000-0002-6484-8655;**

32 **M.C. Román-Martínez. ORCID: 0000-0003-4595-6770**

## 33 1. Introduction

34 The conversion of biomass into fuels and chemicals implies the exploitation of a renewable feedstock and can  
35 contribute to reduce the world's dependence on fossil fuels. There are many studies devoted to promote the use  
36 of biomass with the purpose of achieving a suitable way to replace fossil fuels, contributing as well, to mitigate  
37 the environmental damage caused by their use. An example of these studies can be found in references [1–5].  
38 Nowadays requirements are that the biomass used for such a use must be non-edible and that no agricultural  
39 land is dedicated to biomass growing to avoid interference with food production. Thus, mainly lignocellulosic  
40 biomass by-products from agricultural and industrial processes shall be used. Lignocellulosic biomass is  
41 constituted by the following three polymeric components: cellulose (C6 units (glucose) with 1-4  $\beta$ -glycosidic  
42 bonds), hemicellulose (mainly C5 units (xylose)) and lignin (amorphous polymer with three phenyl propanolic  
43 monomers bound by C-C and ether bonds) [5]. Cellulose, the most abundant component of lignocellulosic  
44 biomass, is considered a particularly attractive resource to obtain fuels and useful chemical products [6] and it  
45 is also frequently used as a model of lignocellulosic materials. Among the several processes for cellulose  
46 conversion into fine chemicals: pyrolysis, microwave cracking, fermentation and hydrolysis, the last one has  
47 shown to be very suitable to obtain important feedstock molecules like glucose or hydroxymethylfurfural [7–  
48 9]. Glucose can be considered as the first molecule obtained from cellulose hydrolysis, and it is an important  
49 product that can be converted into a broad variety of high-added value chemicals (Scheme 1).

50 Compared with other methods, hydrolysis is, in general, less costly and more selective. However, as a  
51 consequence of the robust structure of cellulose due to the profusion of inter and intra-molecular hydrogen  
52 bonds, such a process constitutes a technical and scientific challenge. Cellulose hydrolysis is usually carried  
53 out by means of homogeneous catalysis, either by enzymatic reactions [10] or by acidic hydrolysis using  
54 mineral acids [7]. However, these techniques present important drawbacks like long reaction time, low catalyst  
55 recycling factor, corrosion, etc., and because of that, heterogeneous catalysis using solid acids (e.g., resins,  
56 metal oxides, zeolites) has become an interesting, and much “greener”, alternative [11, 12].

57 Carbon materials have attracted a lot of attention in the field of heterogeneous catalysis. This is due to  
58 interesting and tuneable properties like morphology, porosity and surface chemistry, in addition to chemical  
59 stability in many liquid media and thermal stability in non-oxidising atmospheres. In fact, they have been  
60 frequently used as catalysts and catalysts supports [13]. The presence of Oxygen Functional Groups (OFG) on  
61 the carbon surface, particularly in the case of mesoporous carbons, seems to be beneficial for the adsorption of  
62  $\beta$ -1,4 glucan chains what can help to the cellulose network disintegration. The formation of hydrogen bonds  
63 with the glucan chains promotes the hydrolysis of the glycosidic bonds [14]. Examples of this use of carbon  
64 materials are the work of Shrotri et al. [15] who modified the carbon surface by air oxidation, but added also  
65 diluted HCl to the reaction media to increase the catalyst's activity, and the work of Hara et al. that used  
66 concentrated H<sub>2</sub>SO<sub>4</sub> solution at high temperature to create not only OFG, but also sulfonic groups [14, 16, 17].  
67 This work is focused on the preparation of carbon based catalysts for the hydrolysis of cellulose, using a  
68 commercial commercial mesoporous activated carbon and with the purpose of developing the suitable surface  
69 chemistry by oxidation and sulfonation treatments carried out in liquid phase at room temperature. The main  
70 objective is to create the suitable amount and type of surface functionalities, especially acidic ones, while  
71 retaining the optimum desired textural properties.

72 The used oxidation method consists of a treatment with a saturated aqueous solution of  $(\text{NH}_4)_2\text{S}_2\text{O}_8$  in 1M  
 73  $\text{H}_2\text{SO}_4$  at room temperature. It has been selected because, as indicated by Moreno-Castilla et al. [18, 19], it  
 74 introduces strong acidic groups and, furthermore, it does not significantly modify the textural properties of the  
 75 original activated carbon; and as indicated by Li et al [20] it is non-hazardous, non potentially explosive,  
 76 economical and highly soluble in water. On the other hand, as sulphuric acid is frequently used to develop  
 77 sulfonic groups on the carbon surface [17, 21, 22], the carbon resulting after the treatment with the 1M  $\text{H}_2\text{SO}_4$   
 78 solution at room temperature (the one used in the ammonium persulfate treatment) has been also considered as  
 79 a potential catalyst. It should be pointed out that these conditions are clearly milder than those usually reported  
 80 for such a way to create sulfonic groups (for example, concentrated  $\text{H}_2\text{SO}_4$  at 373 K [22] and 10M  $\text{H}_2\text{SO}_4$  at  
 81 373 K [21]).

82 The adopted surface modification strategies involve mild conditions and thus, they can be regarded as low-cost  
 83 methods. Minute analysis of the surface chemistry has been performed to determine the specific surface  
 84 functionalities that enhance cellulose hydrolysis and selectivity to glucose.

85 Thus, in summary, this work focuses on the development of effective heterogeneous hydrolysis catalysts  
 86 consisting on functionalized carbon materials, as they have properties scarcely exploited yet for this reaction  
 87 (like a suitable porosity and a tuneable surface chemistry). The development of such catalysts is desired for the  
 88 replacement of the commonly used strong liquid acids. This, together with the use of mild conditions for the  
 89 catalysts preparation (with economic and environmental benefits) and the detailed characterization of the  
 90 carbon based catalysts, are the main scientific contributions of this work.

91

92

93

94

95

96

97

98

99

100

101

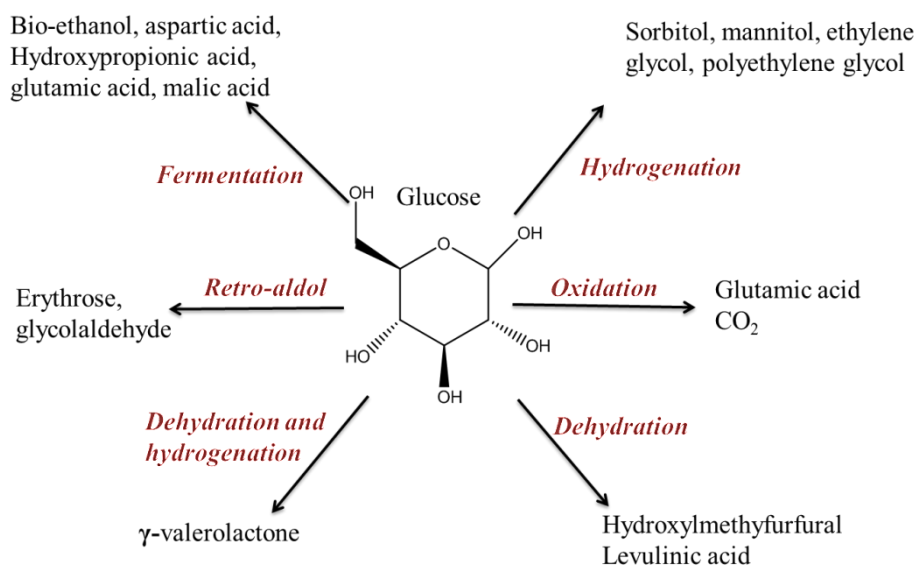
102

103

104

105

106



**Scheme 1.** High added-value chemicals from glucose.

## 107 2. Experimental

### 108 2.1. Materials

109 The commercial activated carbon from MeadWestvaco (USA) named SA-30 which is produced by activation  
110 using  $\text{H}_3\text{PO}_4$  has been selected to prepare the carbon catalyst because of its high surface area and mesopore  
111 volume [23]. The carbon, named only SA in this work, was treatments with the following chemical agents:

112 i) saturated solution of  $(\text{NH}_4)_2\text{S}_2\text{O}_8$  in aqueous  $\text{H}_2\text{SO}_4$  1M (sample SAS)

113 ii)  $\text{H}_2\text{SO}_4$  1M aqueous solution (sample SASu).

114 In both cases, the mixture carbon/solution (1 g activated carbon/ 10 ml solution) was maintained under stirring  
115 for 24 h at room temperature. Afterwards, the treated carbons were filtered, and then washed several times with  
116 distilled water until the filtrate became neutral and sulfates were removed out (determined by  $\text{BaCl}_2$  testing).

117 The performance of the carbon catalysts was compared with that of the Amberlyst 15 resin (Sigma Aldrich), a  
118 known acidic solid [24, 25].

119 The commercial microcrystalline Avicel cellulose (99% purity, Sigma Aldrich) was pre-treated by ball-milling  
120 in a planetary mill, with agate balls/cellulose weight ratio of 3, at 500 rpm for 7 h with reverse rotation every  
121 60 min [26].

### 122 2.2. Characterization

123 The textural properties of SA, SAS and SASu carbon materials were determined by  $\text{N}_2$  adsorption-desorption  
124 at  $-196\text{ }^\circ\text{C}$  using a Quantachrome Autosorb-6B equipment. The apparent BET surface area ( $S_{\text{BET}}$ ) and the total  
125 micropore volume ( $V_{\text{micro}}$ , volume of pores with diameter lower than 2 nm) were calculated using the BET and  
126 Dubinin-Radushkevich equations [27, 28], respectively. The mesopore volume ( $V_{\text{meso}}$ , volume of pores with  
127 diameter between 2 and 20 nm) was estimated as the difference between the amount of  $\text{N}_2$  adsorbed at  
128  $P/P_0=0.99$  and at  $P/P_0=0.2$  and the total pore volume ( $V_{\text{tot}}$ ) was obtained from the volume of  $\text{N}_2$  adsorbed at  
129  $P/P_0=0.95$  [29, 30]. The mean pore size was determined by the equation  $D = 4 \times V_{\text{tot}} / S_{\text{BET}}$  [28].

130 The surface chemistry of the carbon catalysts was analysed by Temperature Programmed Desorption (TPD)  
131 ( $20\text{ }^\circ\text{C}/\text{min}$  up to  $900\text{ }^\circ\text{C}$ ,  $100\text{ ml}/\text{min}$  He flow) using a thermobalance (TA-SDT Q600) coupled to a mass  
132 spectrometer (Thermostar, Balzers). This enables the simultaneous record of weight loss, and  $\text{CO}_2$  and CO  
133 evolution. The surface chemistry of the carbon materials was also characterized by X-ray Photoelectron  
134 Spectroscopy (XPS, VG Microtech Multilab ESCA-3000 spectrometer). XPS spectra were obtained using a  
135 K-Alpha spectrometer (Thermo-Scientific), with a high resolution monochromator and the following  
136 specifications: Al anode ( $1486.6\text{ eV}$ ) X-ray source,  $5 \times 10^{-9}$  mbar analysis chamber pressure and detection in  
137 constant energy mode with pass energy of  $200\text{ eV}$  for the survey spectrum, and of  $50\text{ eV}$  for the sweep in each  
138 individual region. Data analysis was performed with the Origin peak fitting software.

139 Moreover, the amount of acidic sites was determined using a simplified Boehm titration method in which 0.1  
140 g carbon were mixed with 20 ml of a 0.05 M NaOH solution. Then, the mixture was treated in ultrasound bath  
141 for 1 h and, after filtration, the solution was titrated with HCl 0.05 M.

142 The carbon catalysts have been also analysed by TEM in order to characterize their microstructure. JEM-2010  
143 transmission electron microscope from JEOL with an acceleration voltage of 200 kV has been used for this  
144 purpose.

145 The crystallinity of the Avicel cellulose, before and after the milling treatment, was analysed by X-ray  
146 diffraction (XRD) using the Miniflex II Rigaku equipment (30 kV/15 mA) with Cu K $\alpha$  radiation and a scanning  
147 rate of 2°/min, in the 6–80° 2 $\theta$  range. The crystallinity index has been calculated as CrI (%) = [(I<sub>200</sub>-  
148 I<sub>am</sub>)/I<sub>200</sub>]\*100, where I<sub>200</sub> and I<sub>am</sub> are the intensity of the peaks at 22.30° and 18°, respectively [31].

### 149 2.3. Catalytic tests

150 The catalytic tests were performed in a 50 ml stainless steel Parr reactor (Model 4792), lined with a Teflon  
151 container. The reaction conditions were chosen after a literature revision and are the following: 500 mg  
152 cellulose, 125 mg catalyst, 25 ml distilled water, 190°C and 3 h, under stirring. At the end of the experiment,  
153 the solid and liquid phases were separated by filtration. The liquid phase was analysed by high performance  
154 liquid chromatography (HPLC, 1200 infinity Agilent Technologies, column; Hi-Plex Ca (Duo), 300 × 6.5 mm)  
155 and the solid was dried and weighted to calculate the cellulose conversion.

156 Conversion, product yield and selectivity were calculated according to the following expressions:

157  $Conversion = [1 - (\text{weight of unreacted cellulose} / \text{weight of charged cellulose})] \times 100$

158  $Yield\ of\ A = [\text{moles of A} / \text{moles of charged cellulose}] \times 100$

159  $Selectivity\ to\ A = [\text{yield of A} / \text{conversion}] \times 100$

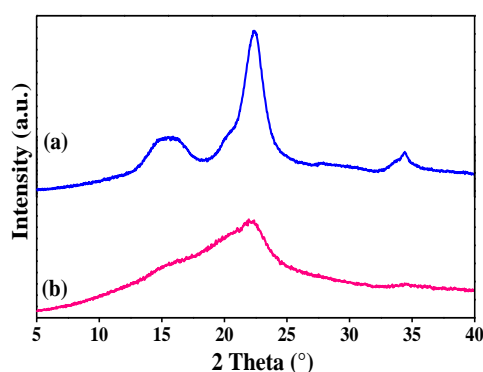
## 160 3. Results and Discussion

### 161 3.1. Cellulose pretreatment

162 Ball milling is an efficient physical pre-treatment to decrease the cellulose crystallinity, thus facilitating its  
163 hydrolysis [32]. Figure 1 shows the XRD results obtained for the original and milled Avicel cellulose, which  
164 reveal the important crystallinity decrease produced after the ball-milling treatment.

165

166



167

168

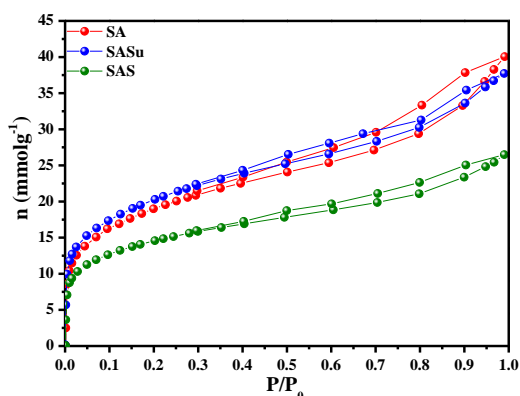
**Fig. 1.** XRD profiles of Avicel cellulose: a) untreated, b) ball-milled.

169

170 The calculated crystallinity index (CrI) of the untreated cellulose (Fig. 1(a)) is 61% while the XRD profile of  
171 the ball-milled cellulose (Fig. 1(b)) does not allow determining the CrI because, as the material becomes quite  
172 amorphous, a clear I<sub>200</sub> peak can not be distinguished. Therefore, it is evident that the ball-milling pretreatment  
173 greatly reduces the crystallinity of this microcrystalline cellulose.

174 3.2. Catalysts textural properties

175 Figure 2 shows the N<sub>2</sub> adsorption-desorption isotherms at -196 °C obtained for the three carbon materials used  
 176 as catalysts. They are type IV isotherms according to the IUPAC classification [30], characteristic of  
 177 mesoporous adsorbents. The relatively high adsorption at low relative pressure indicates that the samples have  
 178 a significant micropore volume, and the steep slope indicates that their pore size distribution is wide. The pore  
 179 size distribution graphs are presented as Supplementary Material (Figure S1) and they show that samples SA  
 180 and SASu have similar pore size distribution while the SAS sample has also a wide pore size distribution but  
 181 with lower narrow micropore volume. The textural parameters, calculated from the N<sub>2</sub> adsorption isotherms as  
 182 indicated in the experimental section, are presented in Table 1.  
 183



184  
 185 **Fig. 2.** N<sub>2</sub> adsorption-desorption isotherms at -196°C.

186 **Table 1.** Textural properties.

187

Sample	S <sub>BET</sub> (m <sup>2</sup> g <sup>-1</sup> )	V <sub>micro</sub> (cm <sup>3</sup> g <sup>-1</sup> )	V <sub>meso</sub> (cm <sup>3</sup> g <sup>-1</sup> )	V <sub>total</sub> (cm <sup>3</sup> g <sup>-1</sup> )	Mean pore size (nm)
SA	1464	0.74	0.73	1.40	3.83
SASu	1522	0.78	0.60	1.24	3.44
SAS	1274	0.56	0.48	0.99	3.11

188  
 189  
 190 S<sub>BET</sub>: BET surface area, V<sub>micro</sub>: micropore volume, V<sub>meso</sub>: mesopore volume, V<sub>total</sub>: total pore  
 191 volume (for details see the text)

192  
 193 The SA activated carbon presents high specific surface area and a well-developed porosity, both in the micro  
 194 and mesopore ranges. The treatment with the H<sub>2</sub>SO<sub>4</sub> 1M solution (sample SASu) produces only a slight  
 195 modification of the porous structure. In contrast, the treatment of SA with the solution of (NH<sub>4</sub>)<sub>2</sub>S<sub>2</sub>O<sub>8</sub> in 1M  
 196 H<sub>2</sub>SO<sub>4</sub> (sample SAS) leads to a significant decrease of the adsorption capacity, which can be due either to  
 197 destruction of pores, or to porosity blockage by the developed surface oxygen groups, as reported for other  
 198 carbon materials submitted to a similar treatment [33].

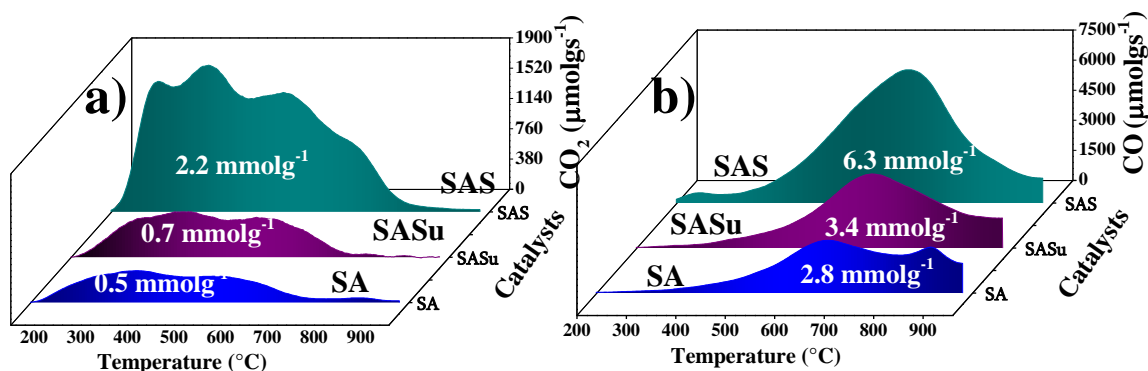
199 In any case, the three carbon materials used in this work present well-developed mesoporosity and high surface  
 200 area. As previously reported [34], mesoporosity is useful for the adsorption of β-1,4 glucan chains, which could  
 201 then be broken on the carbon surface. The Amberlyst 15 resin has low surface area and total pore volume  
 202 (about 40 m<sup>2</sup>g<sup>-1</sup> and 0.2 cm<sup>3</sup>g<sup>-1</sup>, respectively) [24, 25], much lower than those of the carbon materials.

203 The micro/nanostructure of the carbon materials as revealed by TEM can be observed in Figure S2  
 204 (Supplementary Material). It can be seen that it is the expected one for an activated carbon in which the small

205 carbon platelets can be observed forming a microcrystalline structure. It must be mentioned that such a structure  
206 is not significantly modified by the chemical treatments performed.

### 207 3.3. Catalysts surface chemistry

208 Figure 3 shows the CO<sub>2</sub> and CO evolution profiles obtained in the TPD experiments carried out with the three  
209 studied carbon materials. It can be observed that the treatment with 1M H<sub>2</sub>SO<sub>4</sub> leads to the creation of a  
210 moderated amount of oxygen functional groups (OFG) on the carbon surface (sample SASu) while, as  
211 expected, the oxidation treatment carried out to produce the SAS sample results in much higher development  
212 of surface OFG (be aware of the different scale of Figures 3a and 3b). The total amount of CO<sub>2</sub> and CO evolved  
213 in the TPD measurements, calculated as CO+CO<sub>2</sub>, accounts 3.3, 4.1 and 8.5 mmol g<sup>-1</sup> for carbons SA, SASu  
214 and SAS, respectively. The TG data associated to the TPD experiments (Figure S3, Supplementary Material)  
215 show that the mass loss is in agreement with the thermal removal of OFG (comparison of mass loss below  
216 100 °C indicates that sample SASu contained more humidity).



217  
218 **Fig. 3.** TPD spectra of samples SA, SASu and SAS: a) CO<sub>2</sub> evolution and b) CO evolution.

219  
220 In order to perform a deeper characterization of the surface chemistry, the CO<sub>2</sub> and CO evolution profiles  
221 shown in Figure 3 were deconvoluted with the purpose of determining the amount of different types of OFG  
222 (deconvolution is shown in Figure S4 of the Supplementary Material (SM)). For this purpose, deconvolution  
223 was done using a multiple Gaussian function and each peak was centred at temperature values selected  
224 according to the literature [35–37]. The CO<sub>2</sub> evolution peaks corresponding to the decomposition of strongly  
225 (SC) and weakly (WC) acidic carboxylic groups are centred in the 230-270 °C and 360-380 °C intervals,  
226 respectively. Thus, SC and WC are carboxylic groups that differ in their thermal stability and in the pH that  
227 they confer to an aqueous suspension [38]. The TPD peaks due to the decomposition of other functional groups  
228 are centred in the following temperature intervals: ~520-550°C--carboxylic anhydride groups (CA); ~650-  
229 670 °C--lactone groups (LN) at, ~650-700 °C-- phenol type groups (PH) and 750-943°C--carbonyl and quinone  
230 groups (CQ). These temperature intervals reveal that some OFG can decompose showing overlapped CO<sub>2</sub> and  
231 CO desorption peaks.

232 It should be noted that two low temperature CO peaks (labelled as CO#1 and CO#2) appear in the fitting of the  
233 CO evolution profiles. They are centred at temperatures similar to those at which the peaks corresponding to  
234 the decomposition of SC and WC carboxylic groups are located. This phenomenon is also reported in literature.  
235 Figueiredo and co-workers attributed these peaks to the reaction between CO<sub>2</sub> and the carbon surface [39],

236 while Moreno-Castilla et al. consider that the low temperature CO probably comes from carbonyl groups that  
 237 proceed from the decomposition of  $\alpha$ -substituted ketones and aldehydes [18].

238 In the case of the SA carbon, the CO<sub>2</sub> and CO desorption at ~870 °C (see Figure 3 and Figure S4) has been  
 239 explained as due to surface reactions of trace phosphoric groups remaining from the activation treatment with  
 240 H<sub>3</sub>PO<sub>4</sub> [40, 41] The absence of such features in the TPD spectra of SASu and SAS samples would indicate that  
 241 phosphoric groups were mostly eliminated by the treatments with acidic solutions carried out to obtain them  
 242 from the original SA carbon.

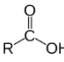
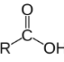
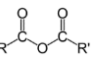
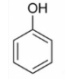
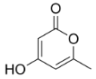
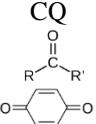
243 The amount of each type of OFG determined from the areas of the deconvoluted TPD profiles (excluding those  
 244 related to phosphoric acid in carbon SA) is presented in Table 2. It can be observed that in the original activated  
 245 carbon, the most abundant OFG are phenol-type groups, followed by carbonyl and quinone groups. The  
 246 treatment with 1M H<sub>2</sub>SO<sub>4</sub> solution leads to the development of all OFG types, being the increase of strongly  
 247 acidic carboxylic groups the most pronounced. The treatment with the saturated solution of (NH<sub>4</sub>)<sub>2</sub>S<sub>2</sub>O<sub>8</sub> in 1M  
 248 H<sub>2</sub>SO<sub>4</sub> produces a noticeable increase in the total amount of OFG, which corresponds to the creation of all  
 249 types of groups. It can be observed that compared to SASu, the SAS carbon contains less carbonyl-quinone  
 250 groups (Table 2).

251 The three samples contain a large amount of acidic OFG (calculated as the sum of SC, WC, CA, PH and LN)  
 252 and the order regarding the OFG content is SA<SASu<<SAS.

253 The acidity of the carbon materials determined by titration (expressed as mmol of acidic sites per gram of  
 254 carbon, Table 2) follows the same trend, although the differences between samples are less pronounced.

255  
 256

257 **Table 2.** Distribution of OFG determined by deconvolution of the TPD profiles and amount of acidic sites  
 258 measured by titration

Sample	OFG (mmolg <sup>-1</sup> )						Total OFG <sup>[a]</sup> (mmolg <sup>-1</sup> )	Acidic OFG <sup>[b]</sup> (mmolg <sup>-1</sup> )	Acidic sites <sup>[c]</sup> (mmolg <sup>-1</sup> )
	SC	WC	CA	PH	LN	CQ			
									
SA	0.06	0.18	0.18	1.02	0.04	0.85	2.33	1.48	3.33
SASu	0.11	0.25	0.25	1.50	0.06	1.33	3.50	2.17	3.44
SAS	0.27	0.82	0.93	3.40	0.22	1.16	6.80	5.64	4.08

[a]: sum of all identified OFG's groups

[b]: sum of SC, WC, CA, PH and LN groups

[c]: measured by titration

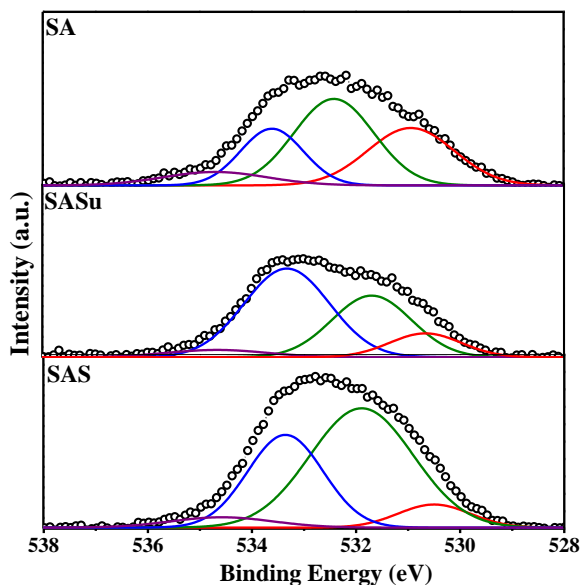
259

260 The amount of acidic OFG determined by deconvolution of the TPD spectra has been plotted versus the amount  
 261 of acidic sites determined by titration, and a linear correlation has been found (Fig. S5, Supplementary  
 262 Material). However, the difference between the total amount of acidic oxygen groups determined from TPD  
 263 data and the acidity determined by titration is relatively large. This point could be explained considering that  
 264 not all the surface functional groups have the same acidity. Thus, titration is the result of an average  
 265 measurement of groups with different acidity and basicity.



266 It can be pointed out that the acidity of carbon SAS ( $4.08 \text{ mmol g}^{-1}$  determined by titration), is comparable to  
267 the acidity of Amberlyst 15 resin ( $4.7 \text{ mmol g}^{-1}$ )[24]. This strong acidity is expected to enhance the catalytic  
268 activity in the hydrolysis of cellulose [14, 42].

269 The surface chemistry of the carbon materials has been also characterized by means of XPS. Figure 4 shows  
270 the O1s XPS spectra of the three studied samples.



271  
272

**Fig. 4.** O 1s XPS data of SA, SASu and SAS

273 Deconvolution of the O1s spectra (Figure 4) based on the binding energy (B.E.) assignments found in the  
274 literature [25, 43, 44] shows peaks centred at the following B.E. values (in eV): i)  $530.7 \pm 0.2$ , assigned to C=O  
275 bond in quinone groups, ii)  $531.8 \pm 0.2$ , related to oxygen in O=C or -OH structures of carbonyl or anhydrides  
276 and hydroxyl groups, iii)  $533.3 \pm 0.2$ , attributed to phenol type groups and iv)  $534.6 \pm 0.2$ , assigned to carboxylic  
277 groups. Table 3 shows the quantification of the O1s spectra in atomic O percentage (At. %) in any of the  
278 mentioned oxygen containing surface functionalities.

279 The contribution of acidic OFG has been calculated assuming that species 2 to 4 (see Table 3) are related with  
280 anhydrides and hydroxyl, phenol, and carboxylic acid groups. It can be observed that the total amount of oxygen  
281 groups, and acidic OFG content determined this way, is similar for SA and SASu samples, and clearly higher for  
282 SAS.

283  
284  
285  
286  
287  
288  
289  
290  
291  
292

293 **Table 3.** O1s XPS data: B.E. (eV), species identification and quantification (At. %).

Element		O 1s (At. %)				Acidic OFG [a]
Species	1	2	3	4		
B.E. (eV)	530.7	531.7	533.3	534.6		
Species	C=O	O=C or -OH	C-OH	C=OOH		
Sample						
SA	2.6	3.6	1.9	0.7	6.2	
SASu	2.9	4.5	0.4	1.0	5.9	
SAS	1.0	7.5	4.3	0.6	12.5	

294 [a] sum of acidic OFG (species 2,3 and 4)

295 The C 1s spectra (presented in Figure S6, Supplementary Material) show, apart from the peak centred at about  
 296 284.5±0.1 eV due to graphitic C=C, other less intense peaks appearing at 286.0±0.1 eV, 286.7±0.1 eV and  
 297 287.5±0.3 eV, which can be attributed to C-O in ether or phenol groups, to quinone or carbonyl groups (C=O),  
 298 and to carboxylic or carboxylic anhydride groups, respectively. Quantification of the C1s spectra has not been  
 299 included, as it will be not precise enough because the intensity of the C1s signals due to OFG is low compared  
 300 to the main peak due to C=C bonds (see Figure S6).

301 The S 2p XPS spectra of samples SASu and SAS, although with a lot of noise, show a peak located at about  
 302 168.1 eV attributed to S in -SO<sub>3</sub>H groups [45]. This means that sulphur is present in these two samples, although  
 303 the amount of this element is very low. In fact, the determination of sulphur by elemental analysis shows that  
 304 the weight concentration of this element in both samples is about 0.1 %. Figure S7 in Supplementary Material  
 305 shows the S 2p XPS spectra of the SAS catalyst before and after the reaction. The profiles obtained are similar,  
 306 which indicates that the -SO<sub>3</sub>H groups have not been leached during reaction.

307 As in the case of the TPD analysis, acidic OFG evaluated by XPS are predominant in all samples (more than  
 308 75% of oxygen atoms are present in acidic groups). This is an interesting property of these carbon materials,  
 309 as the interaction between cellulose β-1,4-glucan chains and acidic OFG on the carbon surface is supposed to  
 310 favour the breakage of the cellulose network, leading to higher catalytic activity [14].

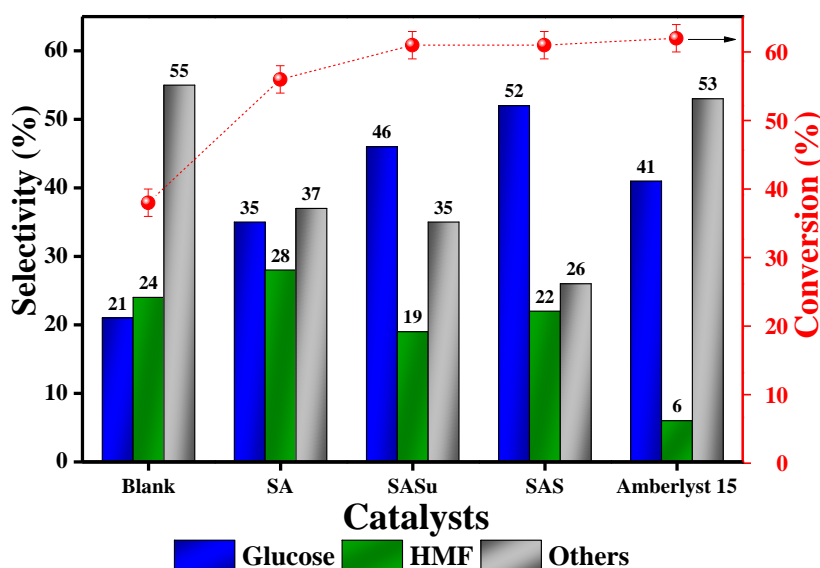
311

### 312 3.4. Catalytic performance

313

314 The hydrolysis of cellulose with the four tested catalysts has led, mainly, to the formation of glucose and  
 315 hydroxymethylfurfural (HMF). As reported in the literature, the reaction starts with a proton from the acid  
 316 catalyst interacting with the glycosidic oxygen atoms that link two sugar units, forming a conjugated acid.  
 317 After addition of water, free sugar and a proton are liberated, and further rehydration and hydrolysis of  
 318 glucose yields HMF [7, 46].

319 The obtained values of cellulose conversion and product selectivity are shown in Figure 5.



321

322

**Fig. 5.** Cellulose conversion (red points) and products selectivity (HMF: Hydroxymethylfurfural) (500 mg cellulose, 125 mg catalyst, 25 ml distilled water, 190°C and 3 h).

323

324

325

326

327

328

329

330

331

332

333

334

335

336

337

338

339

340

341

342

343

344

345

346

347

348

Using the original SA carbon, cellulose conversion significantly increases compared to the blank test (56% vs. 35% conversion), leading as well to a higher selectivity to glucose. This means that this activated carbon is a good catalyst for cellulose hydrolysis. After surface functionalization (samples SASu and SAS), the carbon catalysts improve their catalytic performance, leading to 60% cellulose conversion and glucose selectivity close to 50%. In contrast, the commercial resin Amberlyst 15 exhibits a good cellulose conversion (62%), but a lower selectivity to glucose (41%). Besides, as in the case of the blank experiment, the Amberlyst 15 resin renders a high proportion of other products, each of them in low concentration, that have not been completely identified (furfural, ethylene glycol, polyethylenglycol and levulinic acid can be some of these products), meaning that using this catalyst, the main hydrolysis products (glucose and HMF) are highly degraded.

Regarding the effectiveness of the studied catalysts in terms of glucose yield, the obtained results with the carbon catalysts are 17%, 28% and 32% for SA, SASu and SAS, respectively, while 25% is obtained with Amberlyst 15. The glucose yield of the oxidized carbon materials is higher than that of Amberlyst 15 because they afford a similar cellulose conversion and are clearly more selective to glucose. Thus, the oxidized carbon materials are more effective catalysts than the commercial resin Amberlyst 15. On the other hand, they are more active than the SA original carbon, in spite of having lower pore volume and, in the case of SAS, also lower surface area, what can be attributed to the increase in the amount of acidic surface groups. However, the extensive creation of acidic OFG by the oxidation treatment with the  $(\text{NH}_4)_2\text{S}_2\text{O}_8$  solution in 1M  $\text{H}_2\text{SO}_4$  (SAS sample) does not lead to a further increase of the cellulose conversion respect to the behaviour of the SASu catalyst, and the increase in glucose selectivity is much lower than the increase in the amount of OFG. The increase in selectivity is more pronounced from SA to SASu than from SASu to SAS. This can be explained either by a limit in the positive effect of acidic OFG, by the lower surface area and pore volume, or by a combination of these two reasons. The good catalytic performance of the SASu and SAS carbons for cellulose hydrolysis can be also related with the presence of sulfonic groups (detected by XPS). The stability of those groups was proved by their presence in the SAS catalyst surface before and after reaction (Fig. S4, SM).

349 The obtained results mean that the oxidized carbon materials show a good catalytic performance. However, to  
 350 support this idea, it is necessary to compare the obtained data with recent results on the topic reported in the  
 351 literature. Nevertheless, such a comparison is usually not straightforward because the reaction conditions are  
 352 different, and sometimes the way to express the catalytic activity is different as well. In any case, some reported  
 353 data have been collected in Table 4, indicating the differences in the operation conditions. The reported data  
 354 correspond to the use of carbon materials as catalysts, without acid addition, and water as solvent. Explanations  
 355 and comments on the information presented in the table are given below.

356

357 **Table 4.** Summary of reported results for several carbon based catalysts in hydrolysis reaction conditions  
 358 similar to those used in the present work.

Entry	Catalyst name	S/C <sup>[a]</sup>	T (°C)	T (h)	X <sub>cellulose</sub> (%)	Y <sub>glucose</sub> (%)	Ref.
1	AC BA-475	6.5	180	0.3	96	27	[15]
2	GO-SO <sub>3</sub> H	1	130	8	-	1.4	[47]
3	LDSA	0.25	180	4	-	46-TRS	[48]
4	MPCSA	0.5	150	6	-	58-TRS	[49]
5	R-MCMB-SO <sub>3</sub> H	0.2	140	4	68	66-TRS	[50]
6	G-TsOH	1	170	12	31	16	[51]
7	SAS	4	190	3	60	32	this work

359 [a]: Substrate/Catalyst ratio

360

361 BA-475, an oxidized (air, 475 °C, 3 h) high surface area (1100 m<sup>2</sup>.g<sup>-1</sup>) commercial activated carbon was used  
 362 as catalyst in a mix-milling process with microcrystalline cellulose (entry 1[15]) and, although a high cellulose  
 363 conversion was obtained (with the advantages of high S/C ratio and low reaction time), the glucose yield is  
 364 moderate, meaning that many by-products have been formed. Besides, the oxidation treatment led to 54% burn-  
 365 off, which implies a significant loss of solid. Huang et al. (entry 2 [47]), used a graphene oxide prepared from  
 366 graphite by the harsh Hummers method, and then submitted to a sulfonation treatment (with 98% sulfuric acid).  
 367 The results are poor using water as solvent (data shown in the table), but they noticeably improve when the  
 368 solvent is 1/10 (vol/vol) mixture of water and N-dimethylacetamide. Gan et al. (entry 3[48]) use a lignin derived  
 369 solid acid (LDSA) sulfonated in concentrated sulfuric acid with quite low S/C ratio (high amount of catalyst).  
 370 The results are expressed as yield to total reducing sugars (TRS) and because of that it is not possible to make  
 371 a proper comparison of glucose yield. Data of entry 4 [49] correspond to a solid acid catalyst prepared by the  
 372 co-carbonization of cellulose and PVC (as a way of reusing plastic wastes) and to cellulose pretreated in highly  
 373 concentrated phosphoric acid. The S/C used is low and instead of glucose yield, yield to TRS is presented. In  
 374 the work of Li et al. (entry 5 [50]) the carbon catalyst is based on coal tar pitch mesocarbon mesobeads  
 375 (MCMB) submitted to a sulfonation treatment in concentrated sulfuric acid. Cellulose was previously  
 376 chemically treated, the S/C is very low and the activity results are also presented as yield to TRS. Finally, the  
 377 work of Chen et al. (entry 6 [51]) reports the behaviour of several carbon materials prepared from glucose by  
 378 hydrothermal synthesis and submitted to different treatments. The one indicated in the table shows the best  
 379 behaviour in terms of glucose yield among those studied.

380 The comparison with literature results shows that the carbon catalysts prepared in the present work, particularly  
381 SAS, can be considered among the best ones because they lead to a high cellulose conversion and good glucose  
382 yield, using water as solvent, a relatively high S/C ratio and short reaction time, although the reaction  
383 temperature is somewhat higher. It is important to point out that the SAS carbon leads to the lowest amount of  
384 by-products, being 74% the global selectivity to interesting products (glucose and HMF). Besides, the carbon  
385 catalysts used in this work have been obtained from a commercial activated carbon and the treatments  
386 performed to modify the surface chemistry can be considered mild, in contrast with the more complex and  
387 costly treatments reported in most publications.

388 In summary, the low-cost (mild conditions) modified carbon materials developed in this work combine the  
389 required acidity and suitable textural properties, and because of that, they perform better than the Amberlyst  
390 15 resin and some other carbon materials reported in the literature. Amberlyst 15 has low surface area and  
391 porosity and a high acidity, which promotes side reactions, converting cellulose or glucose to other by-products.  
392 Also, the carbon materials used in this work can be considered advantageous when compared to the resin and  
393 other carbon materials because of their lower price or easier (and cheaper) preparative procedures.

#### 394 **4. Conclusions**

395 Low-cost solid acid catalysts for cellulose hydrolysis have been prepared by the modification under mild  
396 conditions of the surface chemistry of a commercial mesoporous activated carbon. The three studied carbon  
397 catalysts are active for cellulose conversion, and the two oxidized ones show a high selectivity to glucose.  
398 Because of that, they show a better performance (higher glucose yield and less by-products) than the  
399 commercial Amberlyst 15 resin. SAS carbon (prepared by treatment with a saturated solution of  $(\text{NH}_4)_2\text{S}_2\text{O}_8$   
400 in 1M  $\text{H}_2\text{SO}_4$ ) is the most effective of the studied catalysts, leading to 61% cellulose conversion and 52%  
401 selectivity to glucose. This good behaviour can be attributed to a proper combination of high OFG amount and  
402 suitable porosity. Acidic OFG were found to play a key role in improving the catalytic performance of carbon  
403 materials for cellulose hydrolysis and selectivity to glucose, but the presence of a small amount of sulfonic  
404 groups seems to be also relevant.

#### 405 **5. Acknowledgements**

406 The authors thank Ministerio de Ciencia, Innovación y Universidades (RTI2018-095291-B-I00),  
407 GV/FEDER (PROMETEOII/2014/010) and University of Alicante (VIGROB-136) for financial support.  
408 F.-Z. Azar thanks the AECID (research scholarship for development (2015/2016)) the University of  
409 Alicante (cooperation programs for development) for financial support.

#### 410 **6. Conflict of interest**

411 On behalf of all authors, the corresponding author states that there is no conflict of interest.

#### 412 **7. References**

- 413 1. Serrano-Ruiz JC, Dumesic JA (2011) Catalytic routes for the conversion of biomass into liquid  
414 hydrocarbon transportation fuels. *Energy Environ Sci* 4:83–99.  
415 <https://doi.org/10.1039/C0EE00436G>

- 416 2. Kunkes EL, Simonetti DA, West RM, et al (2008) Catalytic Conversion of Biomass to  
417 Monofunctional Hydrocarbons and Targeted Liquid-Fuel Classes. *Science* (80- ) 322:417 LP –  
418 421. <https://doi.org/10.1126/science.1159210>
- 419 3. Stöcker M (2008) Biofuels and Biomass-To-Liquid Fuels in the Biorefinery: Catalytic  
420 Conversion of Lignocellulosic Biomass using Porous Materials. *Angew Chemie Int Ed* 47:9200–  
421 9211. <https://doi.org/10.1002/anie.200801476>
- 422 4. Kamm B, Grüber PR, Kamm M (2015) Biorefineries – Industrial Processes and Products. In:  
423 Ullmann’s Encyclopedya of Industrial Chemistry. Wiley-VCH Verlag GmbH & Co. KGaA,  
424 Weinheim
- 425 5. Zhou C, Xia X, Lin C, et al (2011) Catalytic conversion of lignocellulosic biomass to fine  
426 chemicals and fuels. *Chem Soc Rev* 5588–5617. <https://doi.org/10.1039/c1cs15124j>
- 427 6. Vyver S Van De, Geboers J, Jacobs PA, Sels BF (2011) Recent Advances in the Catalytic  
428 Conversion of Cellulose. *ChemCatChem* 3:82–94. <https://doi.org/10.1002/cctc.201000302>
- 429 7. Fan L, Gharpuray MM, Lee Y-H (1987) Cellulose Hydrolysis. Springer Berlin, Heidelberg
- 430 8. Liu M, Jia S, Gong Y, et al (2013) Effective Hydrolysis of Cellulose into Glucose over  
431 Sulfonated Sugar-Derived Carbon in an Ionic Liquid. *Ind Eng Chem Res* 52:8167–8173.  
432 <https://doi.org/10.1021/ie400571e>
- 433 9. Rinaldi R, Schüth F (2009) Acid Hydrolysis of Cellulose as the Entry Point into Biorefinery  
434 Schemes. *ChemSusChem* 2:1096–1107. <https://doi.org/10.1002/cssc.200900188>
- 435 10. Zhang YHP, Lynd LR (2004) Toward an aggregated understanding of enzymatic hydrolysis of  
436 cellulose: Noncomplexed cellulase systems. *Biotechnol Bioeng* 88:797–824.  
437 <https://doi.org/10.1002/bit.20282>
- 438 11. Rinaldi R, Schüth F (2009) Design of solid catalysts for the conversion of biomass. *Energy*  
439 *Environ Sci* 2:610-626 <https://doi.org/10.1039/b902668a>
- 440 12. Aspromonte SG, Romero A, Boix A V, Alonso E (2019) Hydrolysis of cellulose to glucose by  
441 supercritical water and silver mesoporous zeolite catalysts. *Cellulose* 26:2471–2485.  
442 <https://doi.org/10.1007/s10570-018-2221-5>
- 443 13. Serp P, Figueiredo JL (2009) Carbon Materials for Catalysis. Wiley, New Jersey.
- 444 14. Kitano M, Yamaguchi D, Suganuma S, et al (2009) Adsorption-enhanced hydrolysis of  $\beta$ -1,4-  
445 glucan on graphene-based amorphous carbon bearing SO<sub>3</sub>H, COOH, and OH groups. *Langmuir*  
446 25:5068–5075. <https://doi.org/10.1021/la8040506>
- 447 15. Shrotri A, Kobayashi H, Fukuoka A (2016) Air Oxidation of Activated Carbon to Synthesize a  
448 Biomimetic Catalyst for Hydrolysis of Cellulose. *ChemSusChem* 9:1299–1303.  
449 <https://doi.org/10.1002/cssc.201600279>
- 450 16. Sugauma S, Nakajima K, Kitano M, et al (2008) Hydrolysis of Cellulose by Amorphous Carbon  
451 Bearing SO<sub>3</sub>H, COOH, and OH Groups. *J Am Chem Soc* 130:12787–12793.  
452 <https://doi.org/10.1021/ja803983h>
- 453 17. Nakajima K, Hara M (2012) Amorphous Carbon with SO<sub>3</sub>H Groups as a Solid Brønsted Acid  
454 Catalyst. *ACS Catal* 2:1296–1304. <https://doi.org/10.1021/cs300103k>
- 455 18. Moreno-Castilla C, Carrasco-Marín F, Mueden A. (1997) The creation of acid carbon surfaces by  
456 treatment with (NH<sub>4</sub>)<sub>2</sub>S<sub>2</sub>O<sub>8</sub>. *Carbon* 35:1619–1626. [https://doi.org/10.1016/S0008-  
457 6223\(97\)00121-8](https://doi.org/10.1016/S0008-6223(97)00121-8)

- 458 19. Moreno-Castilla C, Ferro-García M A., Joly JP, et al (1995) Activated carbon surface  
459 modifications by nitric acid, hydrogen peroxide, and ammonium peroxydisulfate treatments.  
460 *Langmuir* 11:4386–4392. <https://doi.org/10.1021/la00011a035>
- 461 20. Li N, Ma X, Zha Q, et al (2011) Maximizing the number of oxygen-containing functional groups  
462 on activated carbon by using ammonium persulfate and improving the temperature-programmed  
463 desorption characterization of carbon surface chemistry. *Carbon* 49:5002–5013.  
464 <https://doi.org/https://doi.org/10.1016/j.carbon.2011.07.015>
- 465 21. Foo GS, Van Pelt AH, Krötschel D, et al (2015) Hydrolysis of Cellobiose over Selective and  
466 Stable Sulfonated Activated Carbon Catalysts. *ACS Sustain Chem Eng* 3:1934–1942.  
467 <https://doi.org/10.1021/acssuschemeng.5b00530>
- 468 22. Fraile JM, García-Bordejé E, Pires E, Roldán L (2014) New insights into the strength and  
469 accessibility of acid sites of sulfonated hydrothermal carbon. *Carbon* 77:1157-1167.  
470 <https://doi.org/10.1016/j.carbon.2014.06.059>
- 471 23. Marco-Lozar JP, Cazorla-Amorós D, Linares-Solano A (2007) A new strategy for germanium  
472 adsorption on activated carbon by complex formation. *Carbon* 45:2519–2528.  
473 <https://doi.org/10.1016/j.carbon.2007.08.020>
- 474 24. Kunin R, Meitzner E, Oline J (1962) Characterization of Amberlyst 15. *IEC Prod Res Dev* 1:140–  
475 144
- 476 25. Siril PF, Cross HE, Brown DR (2008) New polystyrene sulfonic acid resin catalysts with  
477 enhanced acidic and catalytic properties. *J Mol Catal A Chem* 279:63–68.  
478 <https://doi.org/https://doi.org/10.1016/j.molcata.2007.10.001>
- 479 26. Adsuar-García MD (2017) Catalizadores bifuncionales para la hidrogenación hidrolítica de la  
480 celulosa. PhD thesis. University of Alicante
- 481 27. Gregg SJ, Sing KSW (1999) Adsorption, Surface Area and Porosity. Academic Press, New York
- 482 28. Rouquerol F, Rouquerol J, Sing K (1999) Adsorption by powders and porous solids. Principles,  
483 methods and applications., 1st ed. Academia Press, San Diego
- 484 29. Rodríguez-Reinoso F, Linares-Solano A (1989) Chemistry and Physics of Carbon, Vol. 21.  
485 Marcel Dekker, Inc, New York
- 486 30. Thommes M, Kaneko K, Neimark AV, et al (2015) Physisorption of gases, with special reference  
487 to the evaluation of surface area and pore size distribution (IUPAC Technical Report). *Pure Appl*  
488 *Chem* 87:1051–1069
- 489 31. Das K, Ray D, Bandyopadhyay NR, Sengupta S (2010) Study of the properties of  
490 microcrystalline cellulose particles from different renewable resources by XRD, FTIR,  
491 nanoindentation, TGA and SEM. *J. Polym Environ* 18: 355-363.
- 492 32. Avolio R, Bonadies I, Capitani D, et al (2012) A multitechnique approach to assess the effect of  
493 ball milling on cellulose. *Carbohydr Polym* 87:265–273.  
494 <https://doi.org/10.1016/j.carbpol.2011.07.047>
- 495 33. Rufete-Beneite M, Román-Martínez MC, Linares-Solano A (2014) Insight into the  
496 immobilization of ionic liquids on porous carbons. *Carbon* 77:947–957.  
497 <https://doi.org/10.1016/j.carbon.2014.06.009>
- 498 34. Chung P-W, Charmot A, Click T, et al (2015) Importance of Internal Porosity for Glucan  
499 Adsorption in Mesoporous Carbon Materials. *Langmuir* 31:7288–7295.  
500 <https://doi.org/10.1021/acs.langmuir.5b01115>

- 501 35. Figueiredo JL, Pereira MFR, Freitas MMA, Órfão JJM (1999) Modification of the surface  
502 chemistry of activated carbons. *Carbon* 37:1379–1389. [https://doi.org/10.1016/S0008-  
503 6223\(98\)00333-9](https://doi.org/10.1016/S0008-6223(98)00333-9)
- 504 36. Domingo-García M, López Garzón FJ, Pérez-Mendoza MJ (2002) On the characterization of  
505 chemical surface groups of carbon materials. *J Colloid Interface Sci* 248:116–122.  
506 <https://doi.org/10.1006/jcis.2001.8207>
- 507 37. Li N, Ma X, Zha Q, et al (2011) Maximizing the number of oxygen-containing functional groups  
508 on activated carbon by using ammonium persulfate and improving the temperature-programmed  
509 desorption characterization of carbon surface chemistry. *Carbon* 49:5002–5013.  
510 <https://doi.org/10.1016/J.CARBON.2011.07.015>
- 511 38. Boehm H. (2002) Surface oxides on carbon and their analysis: a critical assessment. *Carbon*  
512 40:145–149. [https://doi.org/10.1016/S0008-6223\(01\)00165-8](https://doi.org/10.1016/S0008-6223(01)00165-8)
- 513 39. Figueiredo JL, Pereira MFR, Freitas MMA, Órfão JJM (2007) Characterization of Active Sites on  
514 Carbon Catalysts. *Ind Eng Chem Res* 46:4110–4115. <https://doi.org/10.1021/ie061071v>
- 515 40. Li Y, Zhang X, Yang R, et al (2015) The role of H<sub>3</sub>PO<sub>4</sub> in the preparation of activated carbon  
516 from NaOH-treated rice husk residue. *RSC Adv* 5:32626–32636.  
517 <https://doi.org/10.1039/C5RA04634C>
- 518 41. Valero-Romero MJ, García-Mateos FJ, Rodríguez-Mirasol J, Cordero T (2017) Role of surface  
519 phosphorus complexes on the oxidation of porous carbons. *Fuel Process Technol* 157:116–126.  
520 <https://doi.org/10.1016/j.fuproc.2016.11.014>
- 521 42. Huang Y-B, Fu Y (2013) Hydrolysis of cellulose to glucose by solid acid catalysts. *Green Chem*  
522 15:1095–1111. <https://doi.org/10.1039/C3GC40136G>
- 523 43. Oh YJ, Yoo JJ, Kim Y II, et al (2014) Oxygen functional groups and electrochemical capacitive  
524 behavior of incompletely reduced graphene oxides as a thin-film electrode of supercapacitor.  
525 *Electrochim Acta* 116:118–128. <https://doi.org/10.1016/j.electacta.2013.11.040>
- 526 44. Velo-Gala I, López-Peñalver JJ, Sánchez-Polo M, Rivera-Utrilla J (2014) Surface modifications  
527 of activated carbon by gamma irradiation. *Carbon* 67:236–249.  
528 <https://doi.org/10.1016/j.carbon.2013.09.087>
- 529 45. Russo PA, Antunes MM, Neves P, et al (2014) Solid acids with SO<sub>3</sub>H groups and tunable surface  
530 properties: versatile catalysts for biomass conversion. *J Mater Chem A* 2:11813–11824.  
531 <https://doi.org/10.1039/C4TA02320J>
- 532 46. Xiang Q, Lee EE, Petterson PO, Torget RW (2003) Heterogeneous Aspects of Acid Hydrolysis of  
533 a-Cellulose. *Appl Biochem Biotechnol* 107:505–514
- 534 47. Huang L, Ye H, Wang S, et al (2018) Enhanced hydrolysis of cellulose by highly dispersed  
535 sulfonated graphene oxide. *BioResources* 13:8853–8870
- 536 48. Gan L, Zhu J (2018) A ligning derived carbonaceous acid for efficient catalytic hydrolysis of  
537 cellulose. *J Bioresour Bioprod* 3:166–171 <https://doi.org/10.21967/jbb.v3i4.9>
- 538 49. Yuan S, Li T, Wang Y, et al (2019) Double-adsorption functional carbon based solid acids  
539 derived from copyrolysis of PVC and PE for cellulose hydrolysis. *Fuel* 237:895–902.  
540 <https://doi.org/10.1016/j.fuel.2018.10.088>
- 541 50. Li H-X, Zhang X, Wang Q, et al (2018) Preparation of the recycled and regenerated mesocarbon  
542 microbeads-based solid acid and its catalytic behaviors for hydrolysis of cellulose. *Bioresour*  
543 *Technol* 270:166–171. <https://doi.org/10.1016/j.biortech.2018.09.037>



544 51. Chen G, Wang X, Jiang Y, et al (2019) Insights into deactivation mechanism of sulfonated  
545 carbonaceous solid acids probed by cellulose hydrolysis. Catal Today 319:25-30.  
546 <https://doi.org/10.1016/j.cattod.2018.03.069>

547

548

549

550